

Emulsifier-Free, Organotellurium-Mediated Living Radical Emulsion Polymerization of Styrene: Polymerization Loci

Yukiya Kitayama, Amorn Chaayasat, Hideto Minami, and Masayoshi Okubo*

Department of Chemical Science and Engineering, Graduate School of Engineering, Kobe University, Kobe 657-8501, Japan

Received June 11, 2010; Revised Manuscript Received August 4, 2010

ABSTRACT: The effect of polymerization temperature in emulsifier-free, organotellurium-mediated living radical emulsion polymerization (emulsion TERP) on the control/livingness and particle size distribution was investigated at 50, 60, and 70 °C. The size distribution of obtained particles was significantly affected by the polymerization temperature, that is, nanometer-sized particles at 50 °C, submicrometer-sized ones at 70 °C and both particles at 60 °C were obtained. At 60 °C the molecular weight distribution of the nanometer-sized particles was narrower than that of the submicrometer-sized ones. M_w/M_n at 70 °C was much high (4.6), on the other hand, it was 1.5 at 50 °C and a middle value (2.0) at 60 °C. When the polymerization temperature was changed from 50 to 60 °C during the emulsion TERP, the particle size distribution and control of molecular weight distribution were, respectively, similar to those at 50 °C. From these results, it is concluded that the particle formation by self-assembly nucleation in the early stage of the emulsion TERP is important for the formation of the monomodal nanometer-sized PS particles with good control/livingness.

Introduction

Controlled/living radical polymerization (CLRP), in which nitroxide-mediated living radical polymerization (NMP),^{1–6} atom transfer radical polymerization (ATRP),^{7–14} reversible addition–fragmentation chain transfer (RAFT) polymerization,^{15–17} and iodide-transfer living radical polymerization (ITP)¹⁸ are well-known, has been remarkably developed in the past 15 years.^{19–21} Recently, organotellurium-mediated living radical polymerization (TERP) was discovered by Yamago and co-workers.^{22–26} The mechanistic/kinetic research in a homogeneous system have been reported that TERP proceeded via both activation processes as shown in Scheme 1: thermal dissociation (TD) (a) such as NMP and degenerative transfer (DT) (b) such as ITP, in which below 100 °C, TD mechanism was negligible. The CLRP techniques enable to synthesize various vinyl polymers, which have a narrow molecular weight distribution and a predicted molecular weight, and to design macromolecular architectures such as block, gradient copolymer and star polymer.²⁷

The CLRP maintains a character of conventional radical polymerization as a tolerance for the application to aqueous dispersed systems,^{28,29} and recently much attention has devoted to the application of CLRP to an emulsion polymerization system, which is a general method for industrial applications. Several reports of the application of CLRP to the emulsion polymerization system have been reported, and they exhibited one or more problems such as poor colloidal stability or poor control of the molecular weight distribution.^{30–33} For example in the case of NMP system using TEMPO as a control agent, polymerization temperature was needed above 120 °C, which led the spontaneous initiation of styrene in monomer droplets and obtained micrometer-sized polymer particles. The most difficult point for the application of CLRP to the emulsion polymerization system

(emulsion CLRP) was the transport of the control agent into micelle (polymerizing particles after nucleation) as a polymerization loci. In ATRP and RAFT³⁰ systems, so far because initiator and control agents, were hydrophobic, most of them partitioned in monomer droplets, which resulted in the poor control of the number-average molecular weight.^{30,34–36}

Recently, a novel approach for the application of RAFT polymerization to the emulsion polymerization system (emulsion RAFT) using poly(acrylic acid) (PAA) based RAFT agent as a water-soluble control agent was reported by Hawke and co-workers.³⁷ The water-soluble control agent propagated with hydrophobic monomer in an aqueous medium, resulting in a low molecular weight amphiphilic block copolymer. The amphiphilic block copolymer self-assembled and formed micelles, which solubilize monomer. After that the polymerization proceeded mainly in the micelles at a high rate under controlled condition. The emulsion RAFT was carried out under monomer feed system to prevent from the adsorption of the control agent at the monomer/water interface.

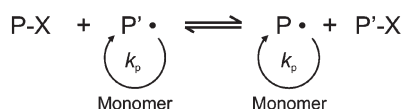
Since then, several papers about emulsion CLRP has been reported and in all cases well-defined vinyl polymers were successfully prepared.^{38–51} Charleux and co-workers developed NMP of *n*-butyl acrylate (BA) and styrene in batch emulsion polymerization using water-soluble alkoxyamine⁵² and emulsion RAFT of BA and MMA (copolymerization with BA) using poly(ethylene oxide) (PEO) based RAFT agent, respectively.⁵³ The PAA and PEO hairy layers worked as stabilizer layer on the particle surfaces. However, abstraction reaction was caused in the hairy layers by several radical species, resulting in midchain radical. The midchain radical underwent the *ss*-scission and formed the hydrophilic radical species, resulting in the secondary nucleation.^{54,55} Moreover, the PEO based nonionic emulsifier partitioned to the monomer phase and monomer-swollen particles.⁵⁶

We have applied TERP of BA to emulsifier-free emulsion polymerization system (emulsion TERP) for the first time by

*Corresponding author. Telephone/Fax: +81-78-803-6161. E-mail: okubo@kobe-u.ac.jp.

Scheme 1. Reversible Activation Process in Organotellurium-Mediated Living Radical Polymerization (X = TeMe in This Work)

(a) Degenerative Chain Transfer (DT)



(b) Thermal Dissociation (TD)



utilizing the self-assembly approach using sodium poly(methacrylic acid)–(PMAA–) methyltellanyl (TeMe) (PMAA₃₀–TeMe) (degree of polymerization of PMAA, 30) at 60 °C, at which TERP proceeds with degenerative chain transfer (DT).⁵⁷ The sodium PMAA₃₀–TeMe is a water-soluble control agent; therefore, the adsorption of the control agent at the monomer/water interface would be suppressed.

In a previous article, it was reported that emulsion TERP of styrene at 60 °C gave a colloiddally stable polystyrene (PS) emulsion with a good livingness.⁵⁸ Except for the final stage (conversion >70%), the number-average molecular weight linearly increased with the conversion. In both cases of BA and styrene the obtained polymer particles had bimodal size distributions comprising submicrometer-sized and nanometer-sized particles under a gentle stirring. Because the nanometer-sized particles had a similar molecular weight and molecular weight distribution as the submicrometer-sized particles, they were not byproduct particles formed in the later stage of the polymerization. However, the particle formation mechanism was unclear.

In this article, in order to understand the particle formation in more detail, the emulsion TERP of styrene will be carried out at different temperatures under gentle stirring.

Experimental Part

Materials. Styrene (Nacalai Tesque, Japan) was purified by distillation under reduced pressure in a nitrogen atmosphere. Deionized water used in all experiments was obtained from Elix UV (Millipore Japan) purification system and had a resistivity of 18.2 MΩ·cm⁻¹. 4,4'-Azobis(4-cyanovaleric acid) (V-501, Wako Pure Chemicals, Japan) was purified by recrystallization in water. PMAA₃₀–TeMe (degree of polymerization of PMAA: 30, M_w/M_n : approximately 1.1) was supplied from Otsuka Chemical Co., Ltd., Osaka, Japan and trimethylsilyldiazomethane (TMSD, Nacalai Tesque) was used as received.

Emulsion TERP of Styrene. A typical procedure is described below. Water and styrene were deoxygenized by nitrogen bubbling. First, an aqueous solution of NaOH (45 g) and V-501 (10.5 mg, 37.8 μmol) were added into a round-bottom Schlenk flask, which was sealed off with a silicon rubber septum and then degassed using several N₂/vacuum cycles, where the amount of NaOH was the same equivalent to that of carboxyl groups of V-501. PMAA₃₀–TeMe (295 μL, 0.127 M aqueous solution neutralized by NaOH, 37.8 μmol) was injected into the system via syringe. After styrene (1.57 g, 15 mmol) was injected via syringe, the flask was then placed in a water bath at 60 °C (taken to be the start of the polymerization, $t = 0$). In all polymerizations, the stirring rate of a magnetic stirrer was fixed at 220 rpm, where most of monomer existed as a layer above the aqueous phase.

Characterization. Conversion was measured by gravimetry. Number- and weight-average molecular weights (M_n and M_w ,

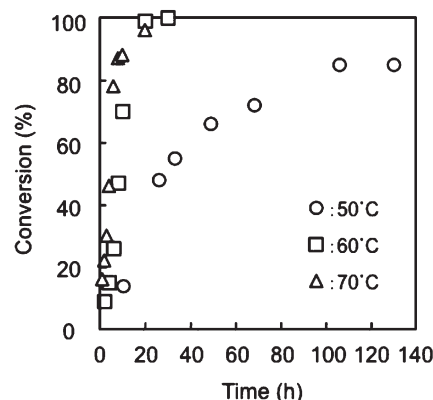


Figure 1. Conversion versus time plots for emulsifier-free, organotellurium-mediated living radical emulsion polymerization (emulsion TERP) of styrene using sodium PMAA₃₀–TeMe and V-501 at 50 °C (circles), 60 °C (squares), and 70 °C (triangles) with 220 rpm stirring. Styrene/PMAA₃₀–TeMe/V-501 (molar ratio) = 400/1/1.

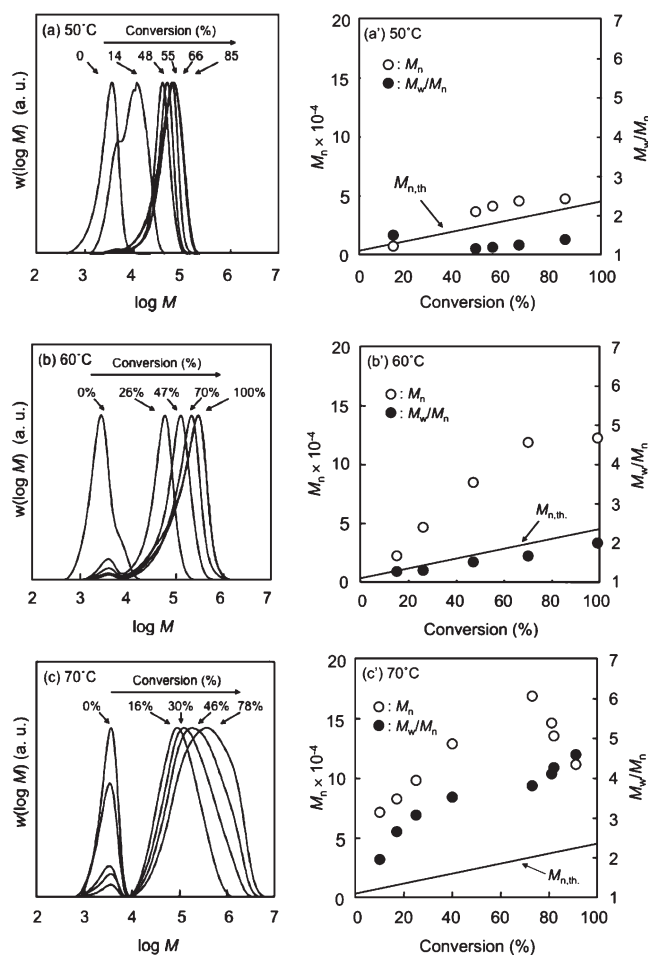


Figure 2. MWD (a, b, c), M_n (open circles) and M_w/M_n (closed circles) (a', b', c') of PMAA₃₀–b-PS–TeMe measured with GPC (detector: refractive index) after methylation of PMAA₃₀ block at different conversions (as indicated in %) of the emulsion TERP using sodium PMAA₃₀–TeMe and V-501 at 50 °C (a, a'), 60 °C (b, b') and 70 °C (c, c') with 220 rpm stirring. Styrene/PMAA₃₀–TeMe/V-501 (molar ratio) = 400/1/1. Full line is $M_{n,th}$.

respectively) and molecular weight distribution (MWD) were measured by GPC using two styrene/divinylbenzene gel columns (TOSOH Corporation, TSKgel GMHHR-H, 7.8 mm i.d. × 30 cm) and THF as an eluent at 40 °C at a flow rate of 1.0 mL/min employing refractive index (RI) (TOSOH RI-8020/21)

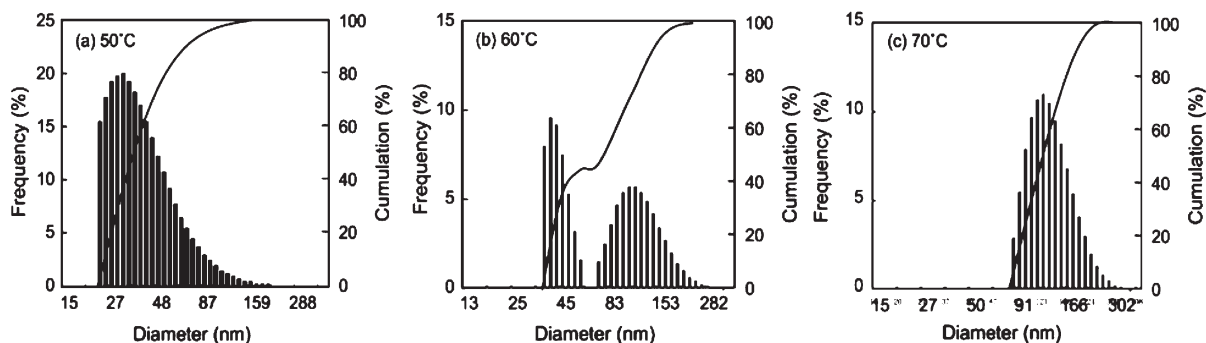


Figure 3. Particle size distributions (by DLS measurements) of PS particles prepared by the emulsion TERP using sodium PMAA₃₀-TeMe and V-501 with 220 rpm stirring at 50 °C (a), 60 °C (b) and 70 °C (c). Styrene/PMAA₃₀-TeMe/V-501 (molar ratio) = 400/1/1. Conversions (%): (a) 85, (b) 100, (c) 96.

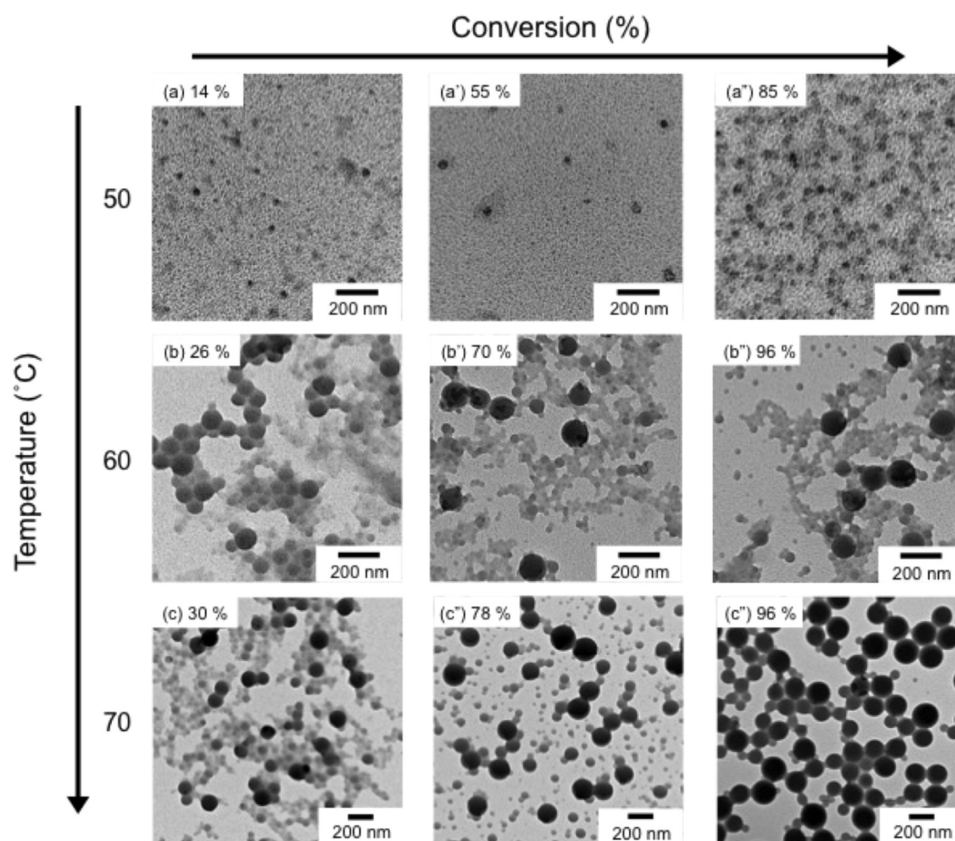


Figure 4. TEM photographs of PS particles prepared at various conversions of the emulsion TERP using sodium PMAA₃₀-TeMe and V-501 at 50 (a, a', a''), 60 (b, b', b''), and 70 °C (c, c', c'') with 220 rpm stirring. Styrene/PMAA₃₀-TeMe/V-501 (molar ratio) = 400/1/1.

and ultraviolet (UV) detectors (TOYO SODA UV-8II). The columns were calibrated with six standard PS samples (1.05×10^3 to 5.48×10^6 , $M_w/M_n = 1.01$ – 1.15). Theoretical molecular weight ($M_{n,th}$) was calculated by following equation:

$$M_{n,th} = MW_{PMAA30-TeMe} + \left(\frac{[M]_0 MW_M \alpha}{[PMAA-TeMe]_0} \right)$$

Here α is the conversion of monomer, $MW_{PMAA30-TeMe}$ and MW_M are the molecular weights of PMAA₃₀-TeMe and styrene, respectively, and $[M]_0$ and $[PMAA_{30}-TeMe]_0$ are the initial concentrations of monomer and PMAA₃₀-TeMe, respectively. Before gel permeation chromatography (GPC) measurement, the polymers were modified by methylation of the carboxyl group of MAA units using TMSD according to the previous work²⁶ as follows. After acidification of the medium, the poly-

mers were recovered by drying polymer emulsion. They were dissolved in a mixture of dimethylformamide and methanol at room temperature. The yellow solution of TMSD was added dropwise at room temperature into the polymer solution and reacted overnight. After excess TMSD was destroyed by acetic acid, the polymer solution was mixed with THF and used for GPC measurement.

Number- and weight-average particle diameters (D_n and D_w , respectively) were measured using a dynamic light scattering (DLS, FPAR-1000 RK, Fiber-optics particle analyzer, Photol Otsuka electronics, Osaka, Japan) at the light scattering angle 90° at room temperature using the Contin analysis routine.⁵⁹ 1–2 droplets of emulsion samples withdrawn from the reactor were diluted with approximately 8 mL of distilled water before measurement in the dilution mode.

Polymer particles were observed with transmission electron microscopy (TEM, JEOL JEM-1230 electron microscope).

Each emulsion was diluted to approximately 50 ppm, and then a drop was placed on a carbon-coated copper grid and dried at room temperature in a desiccator.

Results and Discussion

3.1. Effect of Temperature. Figure 1 shows conversion versus time plots of emulsion TERPs of styrene using sodium PMAA₃₀-TeMe and V-501 at 50, 60, and 70 °C with 220 rpm stirring. The polymerization smoothly proceeded without induction period at each polymerization temperature, and stable PS emulsions were obtained without coagulation. The polymerization rate increased significantly from 50 to 60 °C. From 60 to 70 °C the polymerization rate increased slightly. In emulsion polymerization, it is well-known that the polymerization rate under zero-one system depends on the number of the polymer particles.⁶⁰ As discussed in Figures 3 and 4, the number of the polymer particles increased from 1.1×10^{13} /mL (D_n = ca. 156 nm) at 70 °C to 1.8×10^{15} /mL (D_n = ca. 31 nm) at 50 °C. These results presumed that the polymerization rate would be larger at 50 °C than at 70 °C, however, the actual polymerization rate was contrary. The reason seems to be due to higher propagation rate constant, higher radical concentration due to large particle diameter⁶¹ and higher concentration of monomer in polymerizing particles due to high mobility of monomer in higher polymerization temperature.

Figure 2 shows MWDs, M_n and M_w/M_n values of PS at various conversions of the emulsion TERPs at 50 (a, b), 60 (a', b'), and 70 °C (a'', b''). In all polymerization temperatures, MWDs shifted to higher molecular weight side as the polymerization proceeded and they became narrower with decreasing polymerization temperature. M_n values linearly increased until high conversion and then declined downward

in the final stage of the polymerizations (conversion > 70%), which seems to be caused due to additional chains generated from the initiator and/or unreacted control agent. M_w/M_n value was improved with decreasing polymerization temperature, in which it decreased from 4.6 at 70 °C to 1.4 at 50 °C. These results indicate that the emulsion TERP of styrene proceeded with maintaining a living nature at least except for the final stage of the polymerization in all polymerization temperatures.

As shown in Figure 2, in which MWD was measured with RI detector, a low molecular weight peak ($\log M = 3.5$) remained throughout the polymerizations at all temperatures. The low molecular weight peaks detected at all temperatures and different conversions with a UV detector were smaller than those detected with RI detector at 70 °C. The results indicate that the unreacted control agents and the reacted ones containing a few styrene units coexisted in the low molecular weight peak. This problem will be investigated in detail in the near future.

Figure 3 shows the particle size distributions (weight distribution) from DLS measurement of PS particles at final conversions prepared by the emulsion TERPs at 50 (a), 60 (b), and 70 °C (c). The particle size distribution comprised mainly nanometer-sized particles (< 50 nm) at 50 °C, on the other hand, it did mainly submicrometer-sized ones (> 100 nm) at 70 °C. In the case of 60 °C, the particle size distribution was clearly bimodal, in which both particles coexisted.

Figure 4 shows TEM photographs of PS particles at various conversions prepared by the emulsion TERPs at 50 °C (a, a', a''), 60 °C (b, b', b'') and 70 °C (c, c', c''). At 50 °C obtained PS particles were nanometer-sized and the size distribution was monomodal. The particle size at 85% conversion was in accordance with the result (Figure 3a) by DLS measurement (D_n : ca. 31 nm). At 60 °C the particle size distribution was bimodal comprising submicrometer-sized and nanometer-sized PS particles, which agreed with the result obtained in the emulsion TERP of BA at 60 °C.⁵⁷ DLS analysis indicates that the weight % of the submicrometer-sized and nanometer-sized PS particles were, respectively, 55 and 45 (Figure 3). At 70 °C obtained PS particles mainly consisted of submicrometer-sized particles and a small amount of the nanometer-sized PS particles were observed. These results indicate that the obtained particle size distribution depended on the polymerization temperature. Both nanometer- and submicrometer-sized particles were formed in the early stage of the polymerization, which were confirmed from the TEM photographs at the low conversions.

To examine M_n and M_w/M_n values of fractions of the nanometer- and submicrometer-sized particles at 60 and 70 °C, the original PS emulsions (at the final stage of the polymerization) having broad particle size distribution were separated to fractions of the nanometer- and submicrometer-sized particles by centrifugation, which was confirmed with TEM observation (Figure 5) and DLS measurement (data omitted).

Table 1 shows M_n and M_w/M_n values of the fractionated submicrometer- and nanometer-sized PS particles at 60 and

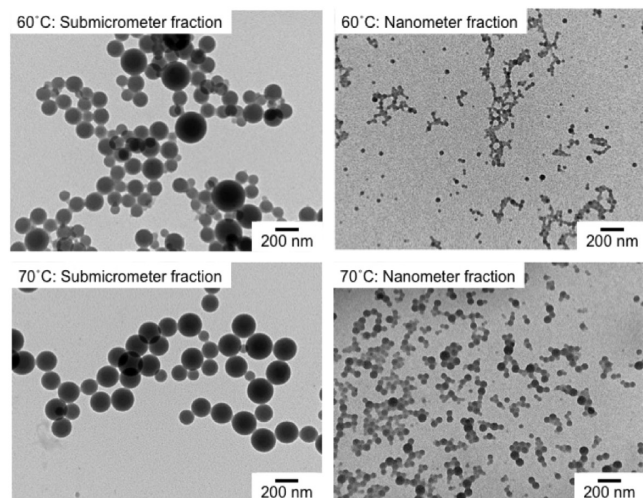


Figure 5. TEM photographs of two centrifugally separated fraction (submicrometer-sized, nanometer-sized) of PS particles prepared by the emulsion TERPs using sodium PMAA₃₀-TeMe and V-501 at 60 (conversion 100%) and 70 °C (conversion 96%).

Table 1. Number-Average Particle Sizes (D_n), M_n , and M_w/M_n Values of Two Centrifugally Separated Fractions of PS Particles, Which Were Prepared by the Emulsion TERP Using Sodium PMAA₃₀-TeMe and V-501 at 60 (Conversion 100%) and 70 °C (Conversion 96%)

polymerization temperature (°C)	size fraction	weight fraction ^a (%)	D_n (nm)	M_n	M_w/M_n
60	submicrometer	55	113	1.4×10^5	2.6
	nanometer	45	35	1.0×10^5	2.4
70	submicrometer	~100	149	1.0×10^5	6.4
	nanometer	~0	52	0.5×10^5	2.7

^a From DLS data shown in Figure 3.

70 °C. At 60 °C, the M_n value of the nanometer-sized particles ($D_n = 35$ nm) was slightly smaller than that of the submicrometer-sized particles ($D_n = 113$ nm), and the M_w/M_n of the nanometer-sized particles was similar to that of the submicrometer-sized particles, indicating that a similar control was undergone in both fractions. On the other hand, at 70 °C, the M_n of submicrometer-sized particles ($D_n = 149$ nm) was significantly larger than that of the nanometer-sized particles ($D_n = 52$ nm). In addition, the M_w/M_n values of the nanometer- and submicrometer-sized particles were 2.7 and 6.4, respectively, that is, there was a great difference.

Figure 6 shows MWDs of fractionated submicrometer- and nanometer-sized PS particles, which were prepared by the emulsion TERP using sodium PMAA₃₀-TeMe and V-501 with 220 rpm stirring at 70 °C. The MWD of the large particles had a shoulder at higher molecular weight side ($>1.0 \times 10^6$), which may be prepared by conventional emulsion polymerization. These results suggest that at 70 °C the different controls proceeded between both fractions. The less control at 70 °C was mainly caused from uncontrolled circumstances in the submicrometer-sized particles.

3.2. Polymerization Loci. Sizes and size distributions of the PS particles obtained by above experiments at 50 °C, 60 and

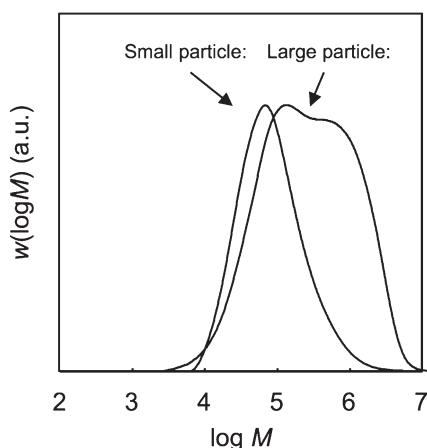


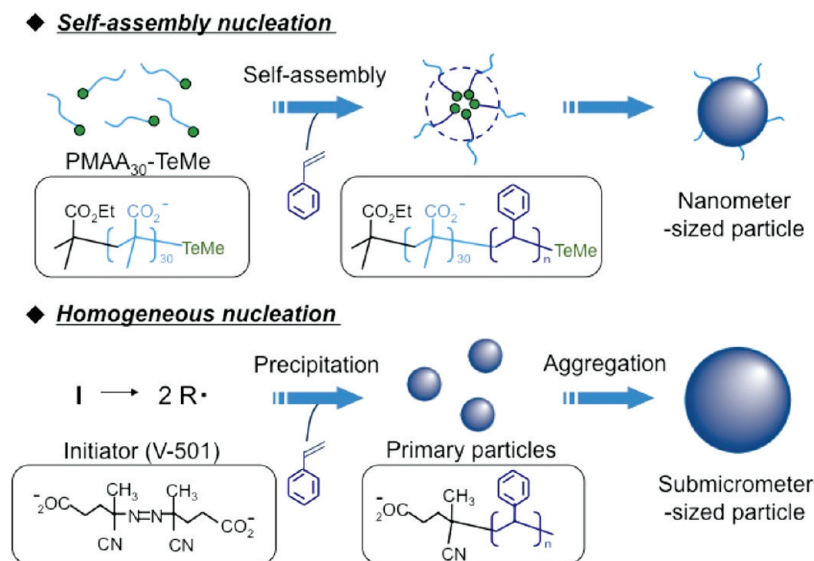
Figure 6. MWDs of fractionated submicrometer- and nanometer-sized PS particles. The original PS particles (conversion: 96%) were prepared by the emulsion TERP using sodium PMAA₃₀-TeMe and V-501 with 220 rpm stirring at 70 °C.

70 °C were obviously different. Except for the polymerization temperature, another polymerization conditions were the same. Elevating polymerization temperature increases radical generation rate of V-501, which would affect the particle formation. Possible particle formation mechanisms in the emulsion TERP are the following two mechanisms: (i) Self-assembly nucleation;⁶² (ii) Homogeneous nucleation.⁶³ Amphiphilic block copolymers formed in the early stage of the polymerization self-assemble, resulting in “micelles”, which solubilize monomer therein. The self-assembled block copolymer “micelle” plays like low molecular weight emulsifier “micelle” in a conventional emulsion polymerization, which works polymerization loci, resulting in a stable nanometer-sized PS particle because of ionized “hairy” surface layer comprising of the sodium PMAA₃₀ block. Homogeneous nucleation is also known in emulsifier-free emulsion polymerization.⁶³ Ionized initiator radicals derived from V-501 above pH > 8 react with monomers dissolving in an aqueous phase up to a certain critical degree of polymerization (J_{crit}) and then precipitate in the aqueous phase when J_{crit} is reached for a given chain, eventually resulting in the formation of primary particles. Because the primary particles do not have PMAA₃₀ hairy layer at the surface, they further aggregate each other, resulting in the submicrometer-sized particles.

In emulsion TERP under DT mechanism, the obtained polymer chains have two types of polymer end groups. One is the PMAA₃₀ group, which is derived from the sodium PMAA₃₀-TeMe, and the other is cyanovaleric acid group, which is derived from V-501 initiator. If relatively large amount of the radicals are generated from the V-501, a large number of oligomers having an ionized cyanovaleric acid end group are generated in the aqueous phase. The oligomer radicals can entry the preformed particles or reach the J_{crit} , leading to the homogeneous nucleation. Therefore, when the polymerization temperature was increased, the formation of the submicrometer-sized particles by homogeneous nucleation must be enhanced (Scheme 2).

3.3. Improving the Control/Livingness. On the basis of the particle formation described above, the suppression of the homogeneous nucleation should give a narrow molecular weight distribution. In order to clarify this, the emulsion TERP was started at 50 °C, and then the polymerization temperature was elevated from 50 to 60 °C after the particle formation in the initial stage of polymerization.

Scheme 2. Particle Formation Mechanisms in the Emulsion TERP of Styrene: (i) Self-Assembly Nucleation; (ii) Homogeneous Nucleation



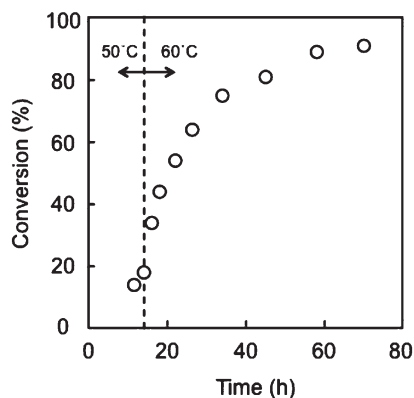


Figure 7. Conversion versus time plot for emulsion TERP of styrene using sodium PMAA₃₀-TeMe and V-501 at 50 °C for 14 h, followed by 60 °C with 220 rpm stirring. Styrene/PMAA₃₀-TeMe/V-501 (molar ratio) = 400/1/1.

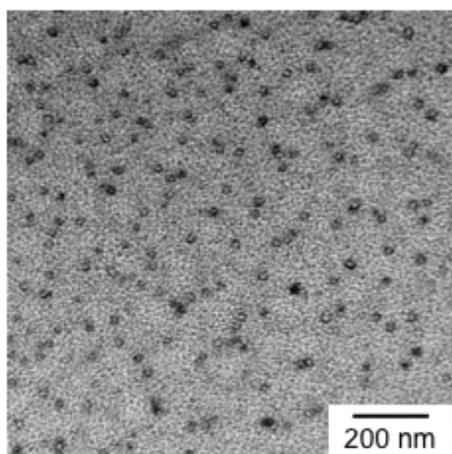


Figure 8. TEM photograph of PS particles (conversion 91%) prepared of the emulsion TERP using sodium PMAA₃₀-TeMe and V-501 with 220 rpm stirring at 50 °C for 14 h, following 60 °C. Styrene/PMAA₃₀-TeMe/V-501 (molar ratio) = 400/1/1.

Figure 7 shows a conversion–time curve of emulsion TERP of styrene using sodium PMAA₃₀-TeMe and V-501 with 220 rpm stirring at 50 °C for 14 h, followed by 60 °C. The polymerization was accelerated by increasing temperature from 50 to 60 °C at 14 h (conversion: ca. 18%). The conversion was reached approximately 90% in 70 h, which was almost half the time of the polymerization at 50 °C. Obtained PS emulsion was very stable and had a similar transparency as that prepared at 50 °C. As will be seen in TEM photograph shown in Figure 8, the size of PS particles in the former case was nanometer, which was the same as that of the latter case.

Figure 9 shows MWDs, M_n and M_w/M_n values of PS particles at various conversions of the emulsion TERP at 50 °C for 14 h (conversion, ca. 18%), followed by 60 °C. The MWD gradually shifted to higher molecular weight side with increasing conversion. Experimental M_n values were slightly differed from $M_{n,th}$, and M_w/M_n values were relatively small (approximately 1.5). Such variations of MWD, M_n and M_w/M_n values with the conversion were in accordance with those prepared by the emulsion TERP not at 60 °C, but at 50 °C (Fig. 9c).

From these results, it is concluded that the particle formation by self-assembly nucleation in the early stage of the emulsion TERP is important for the formation of the

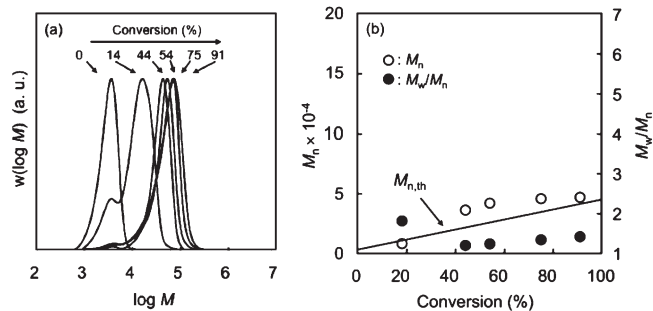


Figure 9. MWD (a), M_n (open circles), and M_w/M_n (closed circles) (b) of PMAA₃₀-b-PS-TeMe measured with GPC (detector: refractive index) after methylation of PMAA₃₀ block at different conversions (as indicated in %) of the emulsion TERP using sodium PMAA₃₀-TeMe and V-501 with 220 rpm stirring at 50 °C for 14 h, followed by 60 °C. Styrene/PMAA₃₀-TeMe/V-501 (molar ratio) = 400/1/1. Full line is $M_{n,th}$.

monomodal nanometer-sized PS particles with good control/livingness.

Acknowledgment. The authors are grateful to Otsuka Chemical Co., Ltd. for supplying organotellurium compounds. This work was partially supported by Grant-in-Aid for Scientific Research (A) (Grant 21245050) from the Japan Society for the Promotion of Science (JSPS) and by Research Fellowships of the Japan Society for the Promotion of Science (JSPS) for Young Scientists (given to Y.K.).

References and Notes

- (1) Georges, M. K.; Veregin, R. P. N.; Kazmaier, P. M.; Hamer, G. K. *Macromolecules* **1993**, *26*, 2987–2988.
- (2) Hawker, C. J.; Bosman, A. W.; Harth, E. *Chem. Rev.* **2001**, *101*, 3661–3688.
- (3) Zetterlund, P. B.; Okubo, M. *Macromolecules* **2006**, *39*, 8959–8967.
- (4) Wakamatsu, J.; Kawasaki, M.; Zetterlund, P. B.; Okubo, M. *Macromol. Rapid Commun.* **2007**, *28*, 2346–2353.
- (5) Alam, M. N.; Zetterlund, P. B.; Okubo, M. *Macromol. Chem. Phys.* **2006**, *207* (19), 1732–1741.
- (6) Aldabbagh, F.; Dervan, P.; Phelan, M.; Gilligan, K.; Cunningham, D.; McArdle, P.; Zetterlund, P. B.; Yamada, B. *J. Polym. Sci., Part A: Polym. Chem.* **2003**, *41*, 3892–3900.
- (7) Kato, M.; Kamigaito, M.; Sawamoto, M.; Higashimura, T. *Macromolecules* **1995**, *28*, 1721–1723.
- (8) Wang, J.; Matyjaszewski, K. *J. Am. Chem. Soc.* **1995**, *117*, 5614–5615.
- (9) Kamigaito, K.; Ando, T.; Sawamoto, M. *Chem. Rev.* **2001**, *101*, 3689–3745.
- (10) Matyjaszewski, K.; Xia, J. *Chem. Rev.* **2001**, *101*, 2921–2990.
- (11) Kagawa, Y.; Zetterlund, P. B.; Minami, H.; Okubo, M. *Macromol. Theory Simul.* **2006**, *15*, 608–613.
- (12) Kagawa, Y.; Minami, H.; Okubo, M.; Zhou, J. *Polymer* **2005**, *46*, 1045–1049.
- (13) Kitayama, Y.; Yorizane, M.; Kagawa, Y.; Minami, H.; Zetterlund, P. B.; Okubo, M. *Polymer* **2009**, *50*, 3182–3187.
- (14) Kagawa, Y.; Kawasaki, M.; Zetterlund, P. B.; Minami, H.; Okubo, M. *Macromol. Rapid Commun.* **2007**, *28*, 2354–2360.
- (15) Chiefari, J.; Chong, Y. K.; Ercole, F.; Krstina, J.; Jeffery, J.; Le, T. P. T.; Mayadunne, R. T. A.; Meijs, G. F.; Moad, C. L.; Rizzardo, E.; Thang, S. H. *Macromolecules* **1998**, *31*, 5559–5562.
- (16) Moad, G.; Chong, Y. K.; Postma, A.; Rizzardo, E.; Thang, S. H. *Polymer* **2005**, *46*, 8458–8468.
- (17) Moad, G.; Rizzardo, E.; Thang, S. H. *Aust. J. Chem.* **2006**, *59*, 669–692.
- (18) Gaynor, S. G.; Wang, J. S.; Matyjaszewski, K. *Macromolecules* **1995**, *28*, 8051–8056.
- (19) Matyjaszewski, K., *Controlled/Living Radical Polymerization: Progress in ATRP, NMP, and RAFT*; American Chemical Society: Washington, DC, 2000.
- (20) Matyjaszewski, K., *Advances in Controlled/Living Radical Polymerization*; American Chemical Society: Washington, DC, 2003.

- (21) Braunecker, W.; Matyjaszewski, K. *Prog. Polym. Sci.* **2007**, *32*, 93–146.
- (22) Yamago, S.; Iida, K.; Yoshida, J. *J. Am. Chem. Soc.* **2002**, *124*, 13666–13667.
- (23) Yamago, S.; Ray, B.; Iida, K.; Yoshida, J.; Tada, T.; Yoshizawa, K.; Kwak, Y.; Goto, A.; Fukuda, T. *J. Am. Chem. Soc.* **2004**, *126*, 13908–13909.
- (24) Yamago, S. *J. Polym. Sci., Part A: Polym. Chem.* **2006**, *44*, 1–12.
- (25) Kwak, Y.; Tezuka, M.; Goto, A.; Fukuda, T.; Yamago, S. *Macromolecules* **2007**, *40*, 1881–1885.
- (26) Sugihara, Y.; Kagawa, Y.; Yamago, S.; Okubo, M. *Macromolecules* **2007**, *40*, 9208–9211.
- (27) Gao, H.; Matyjaszewski, K. *Prog. Polym. Sci.* **2009**, *34*, 317–350.
- (28) Zetterlund, P. B.; Kagawa, K.; Okubo, M. *Chem. Rev.* **2008**, *108*, 3747–3794.
- (29) Cunningham, M. F. *Prog. Polym. Sci.* **2008**, *33*, 365–398.
- (30) Uzulina, I.; Kanagasabapathy, S.; Claverie, J. *Macromol. Symp.* **2000**, *150*, 33.
- (31) Monteiro, M. J.; Hodgson, M.; De-Brouwer, H. *J. Polym. Sci., Part A: Polym. Chem.* **2000**, *38*, 3864–3874.
- (32) Monteiro, M. J.; de-Barbeyrac, J. *Macromolecules* **2001**, *34*, 4416–4423.
- (33) Monteiro, M. J.; Sjöberg, M.; van-der-Vlist, J.; Göttgens, C. M. *J. Polym. Sci., Part A: Polym. Chem.* **2000**, *38*, 4206–4217.
- (34) Monteiro, M. J.; de Barbeyrac, J. *Macromolecules* **2001**, *34*, 4416.
- (35) Prescott, S. W.; Ballard, M. J.; Rizzardo, E.; Gilbert, R. G. *Macromolecules* **2002**, *35*, 5417.
- (36) Prescott, S. W.; Ballard, M. J.; Rizzardo, E.; Gilbert, R. G. *Aust. J. Chem.* **2002**, *55*, 415.
- (37) Ferguson, C. J.; Hughes, R. J.; Nguyen, D.; Pham, B. T. T.; Gilbert, R. G.; Serelis, A. K.; Such, C. H.; Hawket, B. S. *Macromolecules* **2005**, *38*, 2191.
- (38) Nicolas, J.; Charleux, B.; Guerret, O.; Magnet, S. *Angew Chem Int Ed* **2004**, *43*, 6186.
- (39) Nicolas, J.; Charleux, B.; Guerret, O.; Magnet, S. *Macromolecules* **2005**, *38*, 9963.
- (40) Nicolas, J.; Charleux, B.; Magnet, S. *J. Polym. Sci., Part A: Polym. Chem.* **2006**, *44*, 4142–4153.
- (41) Maehata, H.; Liu, X.; Cunningham, M.; Keoshkerian, B. *Macromol. Rapid Commun.* **2008**, *29*, 479–484.
- (42) Simms, R. W.; Hoidas, M. D.; Cunningham, M. *Macromolecules* **2008**, *41*, 1076–1079.
- (43) Dire, C.; Magnet, F.; Couvreur, L.; Charleux, B. *Macromolecules* **2009**, *42*, 95–103.
- (44) Stoffelbach, F.; Tibiletti, L.; Rieger, J.; Charleux, B. *Macromolecules* **2008**, *41*, 7850.
- (45) Ferguson, C. J.; Hughes, R. J.; Pham, B. T. T.; Hawket, B. S.; Gilbert, R. G.; Serelis, A. K.; Such, C. H. *Macromolecules* **2002**, *35*, 9243–9245.
- (46) Ferguson, C. J.; Hughes, R. J.; Nguyen, D.; Pham, B. T. T.; Gilbert, R. G.; Serelis, A. K.; Such, C. H.; Hawket, B. S. *Macromolecules* **2005**, *38*, 2191–2204.
- (47) Sprong, E.; Leswin, J. S. K.; Lamb, D. J.; Ferguson, C. J.; Hawket, B. S.; Pham, B. T. T.; Nguyen, D.; Such, C. H.; Serelis, A. K.; Gilbert, R. G. *Macromol. Symp.* **2006**, *231*, 84–93.
- (48) Hartmann, J.; Urbani, C.; Whittaker, M. R.; Monteiro, M. J. *Macromolecules* **2006**, *39*, 904–907.
- (49) Manguian, M.; Save, M.; Charleux, B. *Macromol. Rapid Commun.* **2006**, *27*, 399–404.
- (50) Ganeva, D. E.; Sprong, E.; Bruyn, H. d.; Warr, G. G.; Such, C. H.; Hawket, B. S. *Macromolecules* **2007**, *40*, 6181–6189.
- (51) dos Santos, A. M.; Pohn, J.; Lansalot, M.; D'Agosto, F. *Macromol. Rapid Commun.* **2007**, *28*, 1325–1332.
- (52) Nicolas, J.; Charleux, B.; Guerret, O.; Magnet, S. *Angew. Chem., Int. Ed.* **2004**, *43*, 6186–6189.
- (53) Rieger, J.; Osterwinter, G.; Bui, C.; Stoffelbach, F.; Charleux, B. *Macromolecules* **2009**, ASAP.
- (54) Thickett, S. C.; Gaborieau, M.; Gilbert, R. G. *Macromolecules* **2007**, *40*, 4710–4720.
- (55) Thickett, S. C.; Morrison, B.; Gilbert, R. G. *Macromolecules* **2008**, *41*, 3521–3529.
- (56) Okubo, M.; Kobayashi, H.; Matoba, T.; Oshima, Y. *Langmuir* **2006**, *22*, 8727–8731.
- (57) Okubo, M.; Sugihara, Y.; Kitayama, Y.; Kagawa, Y.; Minami, H. *Macromolecules* **2009**, *42*, 1979–1984.
- (58) Kitayama, Y.; Chaiyasat, A.; Okubo, M. *Macromol. Symp.* **2010**, *288*, 25–32.
- (59) Provencher, S. W. *Comput. Phys. Commun.* **1982**, *27*, 213–229.
- (60) Smith, W. V.; Ewart, R. H. *J. Chem. Phys.* **1948**, *16*, 592.
- (61) Lau, W.; Westmoreland, D. G.; Novak, R. W. *Macromolecules* **1987**, *20*, 457.
- (62) Ferguson, C. J.; Hughes, R. J.; Nguyen, D.; Pham, B. T. T.; Gilbert, R. G.; Serelis, A. K.; Such, C. H.; Hawket, B. S. *Macromolecules* **2005**, *38*, 2191–2204.
- (63) Fitch, R. M., *Polymer colloids. A comprehensive introduction*; Academic Press: San Diego, CA, 1997.